Proceedings of ISFOG 2025
5TH INTERNATIONAL SYMPOSIUM ON
FRONTIERS IN OFFSHORE GEOTECHNICS
Nantes, France | June 9-13 2025

ISBN 978-2-85782-758-0

Modeling of axially loaded piles using a practical 1D finite element approach

M. Doghman*
College of Engineering and Technology, American University of the Middle East, Egaila 54200, Kuwait

H. Mroueh
University of Lille, IMT Lille Douai, Univ. Artois, Yncrea Hauts-de-France, ULR 4515 - LGCgE, Laboratoire de Génie Civil et géo-Environnement, F-59000 Lille, France

S. Burlon
Terrasol, SETEC, Paris, France

*Mirna.Doghman@aum.edu.kw *(corresponding author)*

ABSTRACT: When subjected to axial loading, the behavior of a pile is analyzed through the assessment of its head load-displacement response. Therefore, an accurate numerical modeling of the soil-pile interface is essential for providing reliable predictions of pile response. This paper introduces an efficient 1D finite element approach, for soil-pile interface modelling which addresses the limitations associated with conventional numerical methods, such as neglecting rheological aspects or requiring time-consuming computations. The modeling of the interface response is done by incorporating a simplified flow rule based on the similarity between the behavior of the soil-pile interface and that of a direct shear test interface. A theoretical pile is considered to compare the results of the developed approach with those from a load-transfer analysis and a 3D analysis using finite difference software (FLAC3D). Findings show that variations in pile mobilized shear stress are governed by the corresponding changes in normal stress along the pile shaft.

Keywords: pile; axial behavior; soil-pile interface; normal stress; 1D finite element approach

1 INTRODUCTION

The behavior of a pile under axial loading is assessed by predicting its bearing capacity and verifying its settlement. The bearing capacity is determined as the sum of the shaft resistance and the base resistance. Like other geotechnical structures, the stability and resistance of pile foundations depend on the soil-structure interaction. Therefore, the analysis of soil-pile interface mechanisms is crucial for effective and economical pile design.

The load-transfer method, commonly known as the t-z curves method, is one of the primary numerical approaches used to investigate the behavior of piles under axial loading. It is implemented using a finite difference scheme. In addition, continuum-based methods, which model the soil as continuous medium, are widely used for pile analysis. These methods are implemented using finite element or finite difference approach.

The first approach initially proposed by Coyle and Reese (1966) is widely favored for its simplicity (Fleming, 1992; Nanda et al., 2014; Li et al, 2020) but it ignores variations in soil normal stresses throughout the pile length and their impacts on the shear behavior. The method relies on pre-established t-z curves to estimate the shear stress for a given displacement, excluding rheological considerations. T-z curves are largely derived from empirical correlations or back-analysis of field test data. While these approaches can be valuable, their applicability outside the specific parameter space of the back-analysis may be uncertain, which can be considered a limitation in modeling the load-settlement behavior of piles. The second approach is applied using both finite element and finite difference methods, which involves implementing an appropriate constitutive model to simulate pile-soil interaction as a continuum (Han et al., 2017; Li et al., 2019). While highly effective, this approach is less commonly used in practical engineering due to its complexity and significant computational requirements.

Numerous constitutive models for the soil-pile interface have been developed based on extensive studies, including laboratory and in-situ experiments under diverse boundary conditions (Fakharian and Evgin, 1997; Mortara et al., 2007; Pra-ai and Boulon, 2016; Ravera and laloui, 2022). A fundamental characteristic of interface shearing is the variation in

normal stress governed by factors such as soil density, shearing level, and interface roughness. This variation, stemming from the dilative or contractive response of the interface (Mascarucci et al., 2016; Lashkari, 2017), significantly affects the maximum shear resistance and the load-bearing capacity of the pile.

This study focuses on the second approach for pile modeling by introducing a 1D finite element approach that accounts for normal stress variation. For this purpose, a suitable constitutive model for the soil-pile interface is proposed, featuring a simplified flow rule. The framework and efficiency of the developed method are addressed. A theoretical pile is used as a case study to evaluate the developed approach by comparing its results with those derived from t-z method and a 3D finite difference analysis conducted using FLAC3D software.

2 CONSTITUTIVE MODEL FOR THE INTERFACE

2.1 Constitutive model formulation

The proposed constitutive model, based on elasto-plasticity principles with a single yield mechanism governed by the Mohr-Coulomb criterion, captures the volumetric behavior of the interface under shear loading, analogous to a direct shear test under constant normal stiffness (CNS).

A non-associated flow rule with a potential function derived from experimental data, based on normal displacement, is employed. These data are extracted from direct shear test experiments conducted under CNS condition. Various physical phenomena, such as contracting phase, dilating phase and stabilization phase, are monitored during monotonic shear loading under CNS condition.

The proposed model is developed within the framework of classical elasto-plastic theory, which involves checking the stress state against the yield criterion for each load increment. Once the plasticity is reached, plastic strains are computed using the flow rule, and stresses and strains are then updated. Usually, when the Mohr-Coulomb criterion with a single mechanism is considered, the plastic multiplier, λ, is calculated using Equation 1:

$$\lambda = \frac{f\left(\sigma_n^f, \tau^f\right)}{\frac{\partial f}{\partial \tau} k_t \frac{\partial g}{\partial \tau} + \frac{\partial f}{\partial \sigma_n} k_n \frac{\partial g}{\partial \sigma_n}} \quad (1)$$

Where, f defines the yield surface, g is the potential function, and σ_n^f and τ^f are the trial normal and shear stress, respectively, meaning the stresses that exceed the yield stress and require correction. Additionally, k_t and k_n represent the shear and normal stiffness of the interface, respectively.

In the proposed model, the flow rule is defined by equation 2:

$$du_n^p = \lambda \frac{\partial g}{\partial \sigma_n} \rightarrow \frac{\partial g}{\partial \sigma_n} = \frac{1}{\lambda} du_n^p \quad (2)$$

Where, du_n^p is the increment of the plastic relative normal displacement derived from experimental curves. Therefore, by substituting $\frac{\partial g}{\partial \sigma_n}$, as defined in Equation 2, into Equation 1, a new formulation of the plastic multiplier is obtained as shown in the following equation:

$$\lambda = \frac{f\left(\sigma_n^f, \tau^f\right) - \frac{\partial f}{\partial \sigma_n} k_n du_n^p}{\frac{\partial f}{\partial \tau} k_t \frac{\partial g}{\partial \tau}} \quad (3)$$

A disturbed relative normal displacement will be applied at the interface nodes, determined from variations in normal displacement, extracted from experimental curves. Trial stresses are adjusted through plastic corrections, based on the values of the plastic multipliers calculated using Equation 3.

The key aspect of the developed model lies in deriving experimental curves that capture the variation in normal relative displacement, which represent the shear paths governing the potential behavior of the interface during shear loading.

2.2 Numerical equation for the experimental curves

A phenomenological formulation is proposed, incorporating various parameters that impact the behavior of the interface. Indeed, the experimental curves, expressed as a function of normal displacement, capture the various physical phenomena that can sequentially occur during monotonic shear loading under CNS condition. These curves are defined as functions of shear displacement, $u_n = f(u_t)$.

This study focuses on representing the different physical phenomena that may alternate during monotonic shear loading under constant normal stiffness condition (CNS), i.e., the contracting phase, the dilating phase, and the stabilization, as can be observed in Figure 1. For this purpose, a modified hyperbolic secant equation, adjusted using a statistical distribution function, is chosen to mathematically describe these various phenomena. This function is presented in Equation 4:

$$u_n = f(u_t) = A\, sech\left(\frac{u_t - B}{2C}\right) + D \quad (4)$$

The selection of the hyperbolic secant function is justified by Figure 2, which illustrates the curve shape described by Equation 4 and clearly represents the alternating physical phenomena listed above. This figure also identifies the parameters *A*, *B*, *C* and *D* listed in Equation 4. The sum of *A* and *D* represents the maximum normal displacement during the contraction phase, denoted as $u_{n,peak}$.

The proposed model includes four parameters calibrated using direct shear test data under conditions of constant normal stiffness and constant normal stress. Experimental results considering various normal stiffness, k_n, and initial normal stress, σ_{n0}, values are used to define each parameter's variation, allowing them to be formulated as functions of k_n and σ_{n0}.

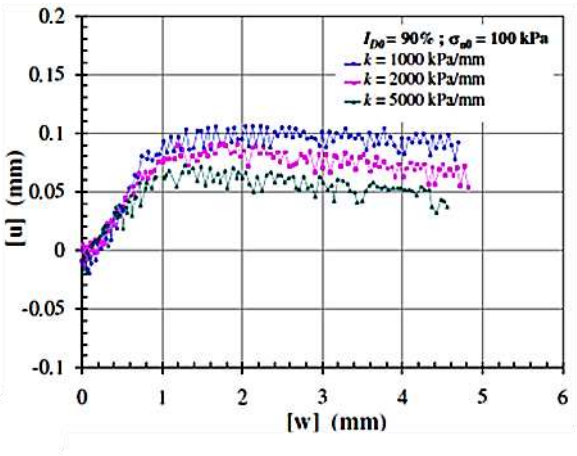

Figure 1. Results of monotonic CNS interface tests with three different values of normal stiffness (k): normal displacement in function of shear displacement (Pra-ai, 2013)

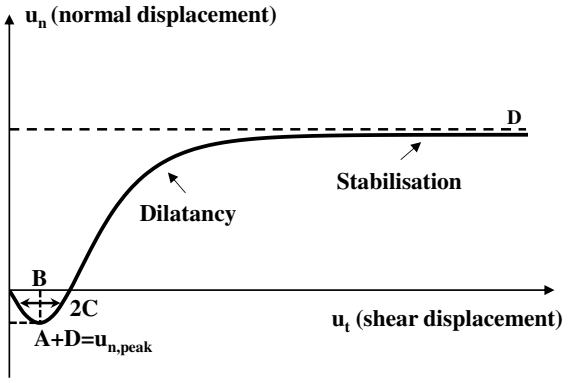

Figure 2. Graphical illustration of Equation 4: $u_n = f(u_t)$

The calibration of the numerical parameters is based on the experimental results from Pra-ai's (2013) thesis under the National SOLCYP Project (2008–2013). The results of monotonic shear tests on dense Fontainebleau sand samples, using rough plates, are used for this purpose. The tests considered different values of k_n (0, 1000 kPa/mm, 2000 kPa/mm, and 5000 kPa/mm) and σ_{n0} (60 kPa, 100 kPa, and 310 kPa). The process of parameter determination is straightforward to implement and is carried out using MATLAB's "Curve Fitting" application. Additional details can be found in Doghman (2021).

3 1D FINITE ELEMENT APPROACH

The aim of this work is to develop a practical approach, using the finite element analysis, and incorporating the impact of normal stress variation on shear behavior along the pile shaft. A total number *n* of 1D finite elements, specifically bar elements with a single degree of freedom (vertical displacement), is used to model the pile. The soil is represented by surface shear springs and surface normal springs to simulate normal stress variation (Figure 3). This approach integrates soil volume changes resulting from shear loading into pile calculation, maintaining a simple bar element formulation while adding a degree of freedom to account for volume variation around the pile. This variation is incorporated as a degree of freedom in the integration of the constitutive law rather than within the bar element itself.

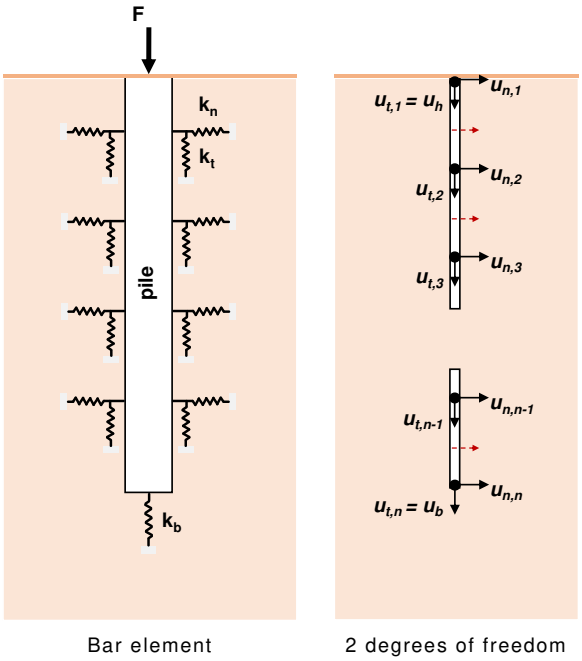

Figure 3. 1D Finite Element Model for Pile Analysis

3.1 Formulation for an element

The problem's variational formulation results in the following equation:

$$[k_p^e]\{u^e\} = [k_p^e]\begin{Bmatrix} u_{t,1}^e \\ u_{t,2}^e \end{Bmatrix} = \{F_{ext}^e\} \qquad (5)$$

Where, $\left[k_p^e\right]$ and $\{u^e\}$ represent the stiffness matrix and the displacement vector of the pile element, respectively, and $\{F_{ext}^e\}$ denotes the external load applied to the pile element. The stiffness matrix $\left[k_p^e\right]$ is determined as follows:

$$\left[k_p^e\right] = \frac{E_{pe}S_e}{h_e}\begin{bmatrix} 1 & -1 \\ -1 & 1 \end{bmatrix} \quad (6)$$

Where, E_{pe} (kPa) is the Young's modulus of the pile element, S_e (m^2) represents its cross-sectional area, and h_e (m) denotes its length.
The external load, $\{F_{ext}^e\}$, comprises two components: one resulting from the applied load at the pile head, $\{F_h^e\}$, and another arising from the shear and normal behavior at the soil-pile interface, along with the base reaction, $\{F_{soil}^e\}$. The latter is described as follows:

$$\{F_{soil}^e\}_t = -k_t^e P_e h_e \begin{bmatrix} 1/3 & 1/6 \\ 1/6 & 1/3 \end{bmatrix} \begin{Bmatrix} u_{t,1}^e \\ u_{t,2}^e \end{Bmatrix} \quad (7)$$

$$\{F_{soil}^e\}_n = -k_n^e P_e h_e \begin{bmatrix} 1/3 & 1/6 \\ 1/6 & 1/3 \end{bmatrix} \begin{Bmatrix} u_{n,1}^e \\ u_{n,2}^e \end{Bmatrix} \quad (8)$$

Where, P_e (m) represents the pile perimeter, while k_t^e and k_n^e (kPa/m) denote the shear and normal stiffnesses of the interface, respectively. $u_{n,1}^e$ and $u_{n,2}^e$ (m) are the normal displacements of the interface at the element nodes. Thus, the following expression can be written:

$$\{F_{soil}^e\} = [k_{soil}^e] \begin{Bmatrix} u_{t,1}^e \\ u_{t,2}^e \\ u_{n,1}^e \\ u_{n,2}^e \end{Bmatrix} \quad (9)$$

The matrices and vectors of each element are assembled into a global system to ensure equilibrium at the nodes. The global system is expressed as:

$$[k]\{U\} = \left[k_p + k_{soil}\right]\{U\} = \{F_h\} \quad (10)$$

The problem is addressed using elasto-plasticity principles. Initially, the elasticity equation is integrated to predict elastic behavior. Subsequently, stresses are adjusted on the yield surface by iteratively correcting the plastic deformation increments. Any plasticity criterion can be implemented.

4 PILE CALCULATION

The developed calculation tool and the proposed interface model are programmed and integrated in Fortran. To assess the performance of the developed approach, the proposed interface model is also explicitly integrated into the finite difference software FLAC3D (Itasca, 2012). Additionally, the t-z method is implemented in Excel VBA.

Tension load is considered in this study to emphasize the impact of normal stress variation on the shear mechanism along the pile shaft.

4.1 Characteristics of the soil and pile for different calculation models

A square concrete pile, with a width D_p = 1 m and a length L = 15 m is analyzed. The Young's modulus is defined as E_p = 20 GPa. For enhanced calculation accuracy, the pile is divided into 30 elements, each measuring 0.5 m in length.

The soil surrounding the pile is dense sand and assumed to be homogeneous. The soil density, γ, is constant and set at 20 kN/m^3. Considering a bored pile, geostatic stress distribution is typically assumed. Therefore, the initial normal stress at the soil-pile interface, σ_{n0}, is determined by the coefficient of earth pressure at rest, K_0. This coefficient is defined as $\nu/(1-\nu)$, where ν is the Poisson's ratio of the soil, taken as 1/3.

The normal stiffness of the interface is determined according to the formula proposed by Baldi at al. (1989), based on a theoretical cone resistance profile that linearly increases with depth. The shear stiffness of the soil-pile interface is set equal to k_n/10.

The friction angle of the interface is set equal to φ = 30° (Pra-ai, 2013). In the t-z calculation, elastic perfectly plastic t-z curves are considered. The ultimate shaft friction is determined using the classical Mohr-Coulomb criterion.

Only one-quarter of the domain is modeled, in the 3D analysis using FLAC3D, due to symmetry (Figure 4). A parametric study was conducted to optimize the mesh, which is illustrated in Figure 4.

The lateral boundaries of the FLAC3D model are normally fixed, and the bottom is fully constrained. Both the pile and soil are modeled as linear elastic elements, with their interaction along the pile shaft represented by interface elements. Table 1 outlines the properties of soil and pile. The pile Poisson's ratio was set to zero to focus on load-transfer mechanisms without lateral deformation effects. A nonzero value may slightly affect lateral stress but has minimal impact on axial load transfer. The load is applied incrementally as vertical displacement at the pile head.

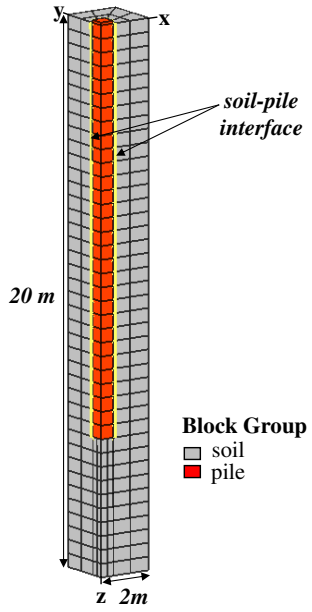

Figure 4. Numerical Model Geometry in FLAC3D

Table 1. Elastic properties of materials used in FLAC3D

Elastic material	Density γ (kN/m^3)	Young's modulus E (GPa)	Poisson's ratio ν
Soil	20	10	1/3
Pile	25	20	0

4.2 Pile response

Figure 5 presents calculation results, in terms of load-head displacement curve, obtained using the classical Mohr-Coulomb criterion, using the t-z method (1D-FDM), and the developed interface model, implemented in both FLAC3D and Fortran. Calculations with the developed 1D tool (1D-FEM), based on the interface model, align well with FLAC3D (3D-FDM) results. Minor differences arise due to the inclusion of soil elements in the 3D analysis. The presence of soil elements in the 3D-FDM model captures lateral confinement effects, and localized variations in stiffness, influencing stress distribution, load transfer mechanisms, and overall pile-soil interaction. This leads to variations compared to 1D models, which provide a more simplified representation of soil behavior. This demonstrates the effectiveness of the developed calculation tool.

The head load-displacement curves generated using the developed model exhibit a non-linear increase as the interface reaches plasticity, eventually attaining a threshold. This behavior is closely linked to the selected numerical equation presented in section 2.2 of this paper (u_n = f (u_t)), which characterizes the dilation phase of the interface response. However, the head load-displacement curve obtained from the t-z calculation does not exhibit the same trend. This calculation does not account for the variation in normal stress along the pile shaft during shearing ($\Delta\sigma_n = 0$).

Figures 6 and 7 compare the mobilized normal stress and shear stress for the upper, middle, and lower pile elements as a function of shear displacement across different calculation approaches. In this context, the upper, middle, and lower pile elements correspond to elements 1, 15, and 30, numbered from top to bottom.

The t-z method does not account for normal stress variation. In contrast, the developed model, incorporating the proposed numerical equation, captures the normal stress variation as demonstrated in both calculations, 3D-FDM and 1D-FEM. The ratio of maximum normal stress to initial normal stress at the end of loading is approximately 8.5 for the upper element, 1.7 for the middle element, and 1.4 for the lower element. It should be noted that the discrepancies between the 3D-FDM and 1D-FEM results, especially at small displacements, are related to the inclusion of soil elements in the 3D analysis.

These figures clearly show that the variation in mobilized shear stress is directly controlled by the corresponding variation in normal stress. Specifically, as the normal stress increases, the shear stress also increases until it reaches a stable value. This correlation highlights the dependency of shear resistance on the normal stress acting at the interface, where higher normal stress leads to greater shear resistance. This effect is particularly evident in the lower pile elements, which experience higher confinement and, consequently, greater shear mobilization. The differences observed across the pile elements demonstrate how stress distribution varies along the pile length, influencing the mobilization of shear resistance.

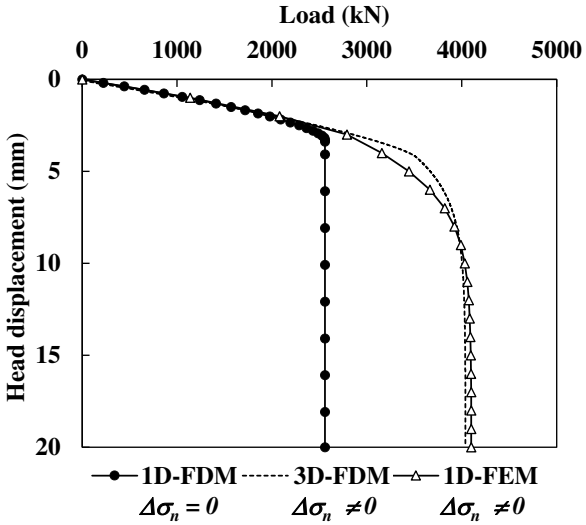

Figure 5. Head load-displacement curves generated by different methods

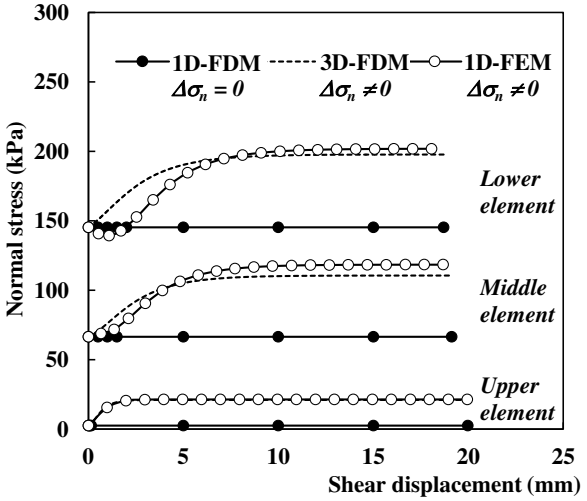

Figure 6. Normal stress in function of shear displacement for different pile elements

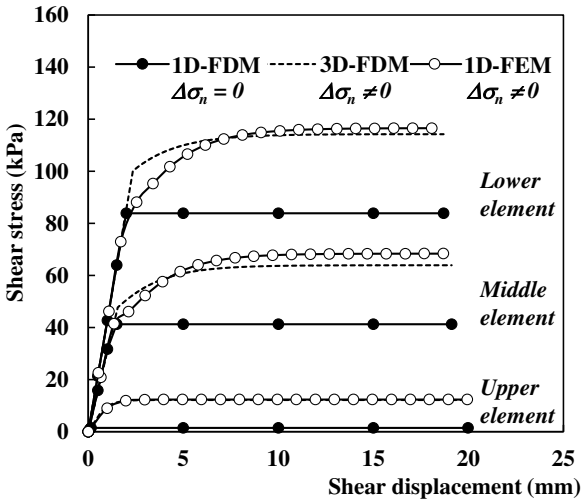

Figure 7. Shear stress in function of shear displacement for different pile elements

5 CONCLUSIONS

This work presents the proposition of an interface model to enhance the soil-pile interface modeling under axial loading. Considering elasto-plasticity principles, the model includes a linear and isotropic elastic part, and a plastic part governed by the Mohr-Coulomb criterion, with a single yield mechanism. A key feature of the model is its flow rule, which directly incorporates volumetric behavior by utilizing experimental data from direct shear tests. These experimental data provide input for normal displacements and stresses, allowing for a direct formulation of flow rule. The hyperbolic secant equation is employed to describe the relationship between normal and shear displacements $u_n = f(u_t)$, capturing contraction and dilatancy during shear loading.

The interface model is implemented in a novel 1D finite element approach, which discretizes the pile into bar elements and solves the problem iteratively while accounting for normal stress variation along the pile shaft by integrating shear and normal springs. To assess the validity of the 1D approach, the interface model is also applied in a 3D finite difference framework using FLAC3D.

The established interface model is evaluated through a 1D calculation using the proposed analysis approach and a 3D finite difference calculation using FLAC3D. The calculation results from these analyses are compared to results from the 1D t-z method to examine the impact of normal stress variation on pile behavior. The dilatancy behavior captured by the interface model leads to an increase in pile capacity, which is highly dependent on the initial normal stress along the pile shaft. The global pile responses from the 1D finite element and 3D analyses show good agreement, though the elastic soil in the 3D model influences the local response at the soil-pile interface. This study demonstrates the ability of the interface model to effectively account for normal stress variation in the shear mechanism along the pile shaft. While the implementation in both 1D and 3D frameworks assesses the validity of the 1D approach, full validation of the model would require comparison with measured pile-head responses.

This paper aims to provide a practical and time-efficient 1D calculation tool for analyzing axially loaded piles, enabling the estimation of displacement and bearing capacity, with potential future application to cyclic axial loading. In terms of computational efficiency under monotonic loading conditions, the 1D-FDM model requires approximately 2 seconds to complete a simulation, whereas the 3D-FDM model can take up to 1 hour. This significant reduction in computation time highlights the advantage of the proposed 1D approach for practical engineering applications. To accommodate cyclic loading, the numerical equation of the constitutive model, derived from experimental curves, would need to be updated to account for the variation in normal displacement at the soil-pile interface during cyclic loading and calibrated using experimental data from cyclic direct shear tests.

AUTHOR CONTRIBUTION STATEMENT

Mirna Doghman: Methodology, Software, Data curation, Formal Analysis, Investigation, Writing-Original draft. **Hussein Mroueh**: Conceptualization, Methodology, Supervision, Funding acquisition,

Writing- Reviewing and Editing. **Sébastien Burlon**: Conceptualization, Methodology, Supervision.

ACKNOWLEDGEMENTS

This work benefitted from France Energies Marines and French National Research Agency (Investments for the Future) funds SOLCYP+: ANR-10-IEED-0006-18.

REFERENCES

Baldi, G., Belloti, R., Ghionna, V.N., Jamiolkowski, M., Lo Presti, D.C. (1989) Modulus of sands from CPTs and DMTs. In: *Proc.12th ICSMFE*, Rio de Janeiro, Brazil, pp. 165–170

Coyle, H.M., Reese, L.C. (1966) Load transfer for axially loaded piles in clay*, J Soil Mech Found Eng Div ASCE*, 92(2), pp. 1–26. https://doi.org/10.1061/JSFEAQ.0000850

Doghman, M. (2021) *Modelling the axial behaviour of marine wind turbine piles anchored in chalk*. PhD thesis, Université de Lille, France

Fakharian, K., Evgin, E. (1997) Cyclic Simple-Shear Behavior of Sand-Steel Interfaces under Constant Normal Stiffness Condition, *Journal of Geotechnical and Geoenvironmental Engineering*, 123, pp. 1096–1105. https://doi.org/10.1061/(ASCE)1090-0241(1997)123:12(1096)

Fleming, W.G. (1992) A new method for single pile settlement prediction and analysis, *Géotechnique*, 42(3), pp. 411–425. https://doi.org/10.1680/geot.1993.43.4.615

Han, F., Salgado, R., Prezzi, M., Lim, J. (2017) Shaft and base resistance of non-displacement piles in sand, *Comput Geotech*, 83, pp. 184–197. https://doi.org/10.1016/J.COMPGEO.2016.11.006

Itasca (2012) FLAC3D Version 5.0. Theory and Background. Itasca Consulting group, Inc., Minnesota, USA

Lashkari, A. (2017) A simple critical state interface model and its application in prediction of shaft resistance of non-displacement piles in sand, *Comput Geotech*, 88, pp. 95–110. https://doi.org/10.1016/j.compgeo.2017.03.008

Li, L., Chen, S.L., Zhang, Z.J. (2019) A numerical study on installation effects and long-term shaft resistance of pre-bored piles in cohesive soils, *Transp Res Rec*, 2673(3), pp. 494–505. https://doi.org/10.1177/0361198119835505

Li, L., Chen, S.L., Zhang, Z.J. (2020) Practical analytical approach for estimating long-term and set-up shaft resistance of prebored piles, *J Geotech Geoenviron Eng*, 146(10). https://doi.org/10.1061/(ASCE)GT.1943-5606.0002354

Mascarucci, Y., Miliziano, S., Mandolini, A. (2016) 3M analytical method: evaluation of shaft friction of bored piles in sands, *J Geotech Geoenviron Eng*, 142(3). https://doi.org/10.1061/(ASCE)GT.1943-5606.0001392

Mortara, G., Mangiola, A., Ghionna, V.N. (2007) Cyclic shear stress degradation and post-cyclic behaviour from sand–steel interface direct shear tests, *Can Geotech J*, 44, pp. 739–752. https://doi.org/10.1139/t07-019

Nanda, S., Patra, N.R. (2014) Theoretical load-transfer curves along piles considering soil nonlinearity, *J Geotech Geoenviron Eng*, 140(1), pp. 91–101. https://doi.org/10.1061/(ASCE)GT.1943-5606.0000997

Pra-ai, S. (2013) *Behaviour of soil-structure interfaces subjected to a large number of cycles. Application to piles*. PhD thesis,Université de Grenoble, France

Pra-ai, S., Boulon, M. (2016) Soil–structure cyclic direct shear tests: a new interpretation of the direct shear experiment and its application to a series of cyclic tests, *Acta Geotech*, 12, pp. 107–127. https://doi.org/10.1007/s11440- 016-0456-6

Ravera, E., Laloui, L. (2022) Failure mechanism of fine-grained soil-structure interface for energy piles, *Soils and Foundations*, 62(3). https://doi.org/10.1016/j.sandf.2022.101152